Nearfield Hydrodynamic Interactions of Ships in Shallow Water

Ronald W. Yeung* and Wei-Yuan Hwang†
Massachusetts Institute of Technology, Cambridge, Mass.

The hydrodynamic interactions of two vessels moving at the same speed in nearfield is considered by applying the slender-body theory. It is shown that, for a water depth that is the same order as the beam of the vessel, the problem reduces to a sequence of inner problems in the cross-flow plane. This reduction to strip-theory allows one to obtain the solution without the necessity of solving an outer problem. Applications were made to two pairs of ship models. Theoretical predictions generally are high as compared with available experimental measurements, but offer a fairly satisfactory qualitative description of the interaction phenomomon when the length of the overlap of the vessels is large as compared with the separation.

1. Introduction

THIS paper addresses the problem of hydrodynamic interactions of ships in shallow water. Thus, it falls into a category of problems brought forth by the advent of large-size vessels, which makes the consideration of restricted-water effects important. Such a category also is characterized by low operation speeds, particularly in harbor or in channels, whereby the leading-order hydrodynamic forces are those associated with fluid inertia instead of the free-surface or viscosity. Therefore, it is hoped that the present theory, which exploits the rigid-free-surface condition, gives sufficiently accurate predictions that could be used for control system design for proximity operations.

In addition to the usual slender-body assumption, it is assumed that the lateral separation between the vessels is small. Further, the water depth is taken to be the same order as the beams. Since only the steady-state problem is considered, this theory may be regarded as complementary to one presented by Tuck and Newman,[1] which requires that the separation distance and water depth are of the order of a ship length. Hence, in contrast to Tuck and Newman and Wang,[2] the present theory, being a nearfield one, requires a detailed knowledge of the hull geometry, and accounts for it accordingly. The slenderness assumption allows the construction of the solution by solving a sequence of two-dimensional problems.

The stated problem can, of course, be solved by a three-dimensional singularity-distribution method (cf., Nowacki[3]). This was, in fact, carried out in part by Norrbin,[4] who found that the computation costs were prohibitively expensive. Other theories related to shallow-water interaction have been given by Collatz,[5] Tuck and Newman[1] (Sec. 4), and Dand,[6] all utilizing two-dimensional theory in the horizontal plane. From these results, it appears that good quantitative predictions for realistic forms would be possible only if the presence of the under-keel clearance is accounted for.

2. Problem Formulation

Consider two vessels moving at the same speed U in water of depth h, as shown in Fig. 1. Since the flow is steady, it is convenient to establish a common reference system midway between the centerplanes of the two ships. At the outset we assume that the free surface can be approximated by a plane and the flow is potential. The disturbance velocity potential ϕ then satisfies the following "exact" conditions:

$$\nabla^2\phi(x,y,z)=0 \tag{1}$$

$$\frac{\partial\phi}{\partial n}\bigg|_{B_1}=U(n_x)_1 \qquad \frac{\partial\phi}{\partial n}\bigg|_{B_2}=U(n_x)_2 \tag{2}$$

$$\frac{\partial\phi}{\partial n}\bigg|_{z=\pm h}=0 \tag{3}$$

where B_1 and B_2 represent the underwater hull surfaces and their reflections about $z=0$. Subscripted Cartesian variables will be used to designate the vessel under consideration. The problem as defined by Eqs. (1-3) represents the three-dimensional flow about two bodies located between parallel plates. Although this could be solved numerically by a surface-singularity-distribution method,[7] we use instead matched asymptotics to obtain the solution of the problem.

Let ϵ be a small parameter representing the body lateral dimensions to the body length. The hull function of the jth body therefore can be described by $r_j(x,\theta)=\epsilon R_j(x,\theta)$, where R_j is 0(1). The lateral separation between bodies d_c and the water depth h are assumed to be $0(\epsilon)$. Furthermore, the ratio of the under-keel clearance to the body radius is assumed to be 0(1). An outer expansion now can be written as follows:

$$\phi=\epsilon\phi^{(1)}(x,y)+\epsilon^2\phi^{(2)}(x,y)+\ldots \tag{4}$$

where, as indicated by Tuck,[8] the shallowness assumption leads to the fact that $\phi^{(i)}$, $i=1,2$, satisfies Laplace's equation in the horizontal plane

$$\left(\frac{\partial^2}{\partial x^2}+\frac{\partial^2}{\partial y^2}\right)\phi^{(i)}(x,y)=0 \qquad i=1,2 \tag{5}$$

By introducing inner variables, $Y=y/\epsilon$, $Z=z/\epsilon$, etc., one can obtain an inner expansion as follows:

$$\Phi(x;Y,Z)=\epsilon f_1(x)+\epsilon^2\Phi^{(2)}(x;Y,Z)+\epsilon^3\Phi^{(3)}(x;Y,Z)+\ldots \tag{6}$$

where the second-order potential satisfies

$$\left(\frac{\partial^2}{\partial Y^2}+\frac{\partial^2}{\partial Z^2}\right)\Phi^{(2)}(x;Y,Z)=0 \tag{7}$$

$$\frac{\partial\Phi^{(2)}}{\partial N}\bigg|_{S_j}=U\frac{\partial}{\partial x}R_j(x,\theta)\Big/\left[1+\left(\frac{(R_j)_\theta}{R_j}\right)^2\right]^{1/2}\equiv U(v_n)_j$$

$$j=1,2 \tag{8}$$

Received Nov. 3, 1976; revision received May 9, 1977.
Index categories: Hydrodynamics; Marine Hydrodynamics, Vessel and Control Surface.

*Assistant Professor, Department of Ocean Engineering.
†Graduate Student, Department of Ocean Engineering.

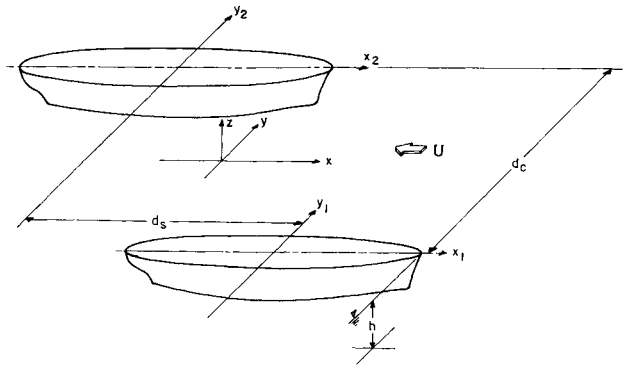

Fig. 1 Coordinate systems and notations.

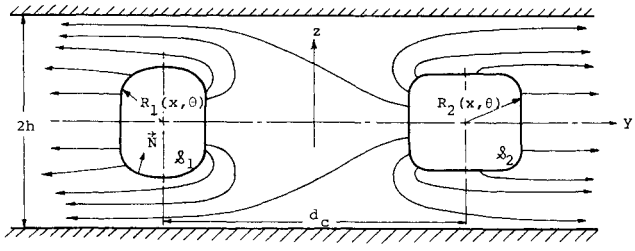

Fig. 2 Two-body problem in the cross-flow plane.

$$\frac{\partial \Phi^{(2)}(x;Y,\pm H)}{\partial Z} = 0 \tag{9}$$

Here N is an interior normal to the cross-sectional curve S_j. The fact that $\Phi^{(1)}$ in Eq. (6) is a function of x only is a consequence of $\Phi_N^{(1)} = 0$ on S_j, $j = 1,2$. Figure 2 illustrates the boundary-value problem for $\Phi^{(2)}$. Note that, at a given section, S_1 and S_2 will not necessarily have the same shape. The boundary-value problem for $\Phi^{(3)}$ can be shown to be

$$\left(\frac{\partial^2}{\partial Y^2} + \frac{\partial^2}{\partial Z^2}\right)\Phi^{(3)}(x;Y,Z) = -f_1''(x) \tag{10}$$

$$\frac{\partial \Phi^{(3)}}{\partial N}\bigg|_{S_j} = -f_1'(x)(v_n)_j \qquad j=1,2 \tag{11}$$

$$\frac{\partial \Phi^{(3)}(x;Y,\pm H)}{\partial Z} = 0 \tag{12}$$

where the prime denotes differentiation with respect to x. In the preceding equations, and in the analysis to follow, all capitalized quantities are by assumption 0(1) in the *inner* field. It is worthwhile to note that neither the outer nor the inner problems, as defined, are complete by themselves; the former lack the body boundary condition, and the latter a condition at infinity.

3. Inner and Outer Solutions and Matching

Consider the problem for $\Phi^{(2)}$. The flux into the fluid $Q^{(2)}$ is given by the rate of change of sectional areas:

$$Q^{(2)} = -\sum_{j=1}^{2}\int_{S_j} ds\frac{\partial \Phi^{(2)}}{\partial N} = -U\sum_{j=1}^{2}\frac{dA_j(x)}{dx} \equiv -UA'(x) \tag{13}$$

where $A_j(x)$ is the sectional area of the jth ship. However, it is not known *a priori* to what extent the flux will be split unevenly. This fact can be incorporated by decomposing $\Phi^{(2)}$ into two component problems, as follows:

$$\Phi^{(2)} = U\phi_0 + V^{(2)}(x)\phi_1 + f_2(x) \tag{14}$$

with

$$\frac{\partial \phi_0}{\partial N}\bigg|_{S_j} = v_n \qquad j=1,2 \tag{15a}$$

$$\lim_{Y\to\pm\infty}\phi_0 = \pm[(-A'/4H)Y + C_0(x)] \tag{15b}$$

and

$$\frac{\partial \phi_1}{\partial N}\bigg|_{6S_j} = 0 \qquad j=1,2 \tag{16a}$$

$$\lim_{Y\to\pm\infty}\phi_1 = Y \pm C_1(x) \tag{16b}$$

where the subscripted ϕ's bear no relation to the superscripted ϕ introduced earlier.

Equations (15) and (16) are of course to be satisfied in conjunction with Eqs. (7) and (9). Thus, ϕ_0 represents a particular solution with an evenly split flux, and ϕ_1 a homogeneous solution corresponding to unit lateral flow. C_0 and C_1 are blockage constants, determinable either analytically or by the numerical solution of ϕ_0 and ϕ_1. The order of magnitude of C_0 and C_1 may be inferred by applying Green's theorem to the potentials ϕ_0 and ϕ_1, respectively. In Sec. 5, it is shown that C_0 is $0(\epsilon^2)$, to the *outer* field, whereas C_1 is $0(\epsilon)$. Since $\Phi^{(2)}$ as defined by Eq. (14) is the term associated with ϵ^2, we observe that the decomposition defined by Eq. (14) contains the tacit assumption that $V^{(2)}$ is $0(\epsilon)$. The unknown functions $V^{(2)}(x)$ and $f_2(x)$ can be determined only by matching with the outer solutions.

It is convenient to regroup the terms of $\Phi^{(2)}$ as even and odd parts, which behave asymptotically as follows:

$$\left.\begin{aligned}\Phi^{(2)}_{\text{even}} &\to \frac{Q^{(2)}}{4H}|Y| + f_2(x) \qquad (17)\\ \Phi^{(2)}_{\text{odd}} &\to V^{(2)}Y + \text{sgn}(Y)[UC_0 + V^{(2)}C_1] \qquad (18)\end{aligned}\right\} \text{as } |Y|\to\infty$$

where sgn is the sign function. For the third-order problem $\Phi^{(3)}$, a similar decomposition to that of $\Phi^{(2)}$ is possible. In fact, $\Phi^{(3)}$ can be written in terms of the previously defined Φ_0 and ϕ_1 in the following form:

$$\Phi^{(3)} = -f_1'[\phi_0 + (V^{(2)}/U)\phi_1] - \tfrac{1}{2}f_1''Y^2 + f_1''\phi_* + V^{(3)}\phi_1 + f_3(x) \tag{19}$$

where f_3 and $V^{(3)}$ are new unknown functions, and ϕ_* corresponds to a problem similar to ϕ_0, but subject instead to the body boundary-condition

$$\frac{\partial \phi_*}{\partial N}\bigg|_{S_j} = Y(N_Y)_j \qquad j=1,2 \tag{20a}$$

and

$$\lim_{Y\to\pm\infty}\phi_* = \pm\frac{A(x)}{4H}|Y| \pm C_*(x) \tag{20b}$$

with C_* being another blockage constant.

Turning now to the outer problem, we note that, since d_c is assumed to be $0(\epsilon)$, the two ships collapse onto the x axis. Equation (5) and the unsymmetrical nature of the flow about the $x-z$ plane suggest an outer representation by distributing two-dimensional sources and vortices. Thus, we write

$$\epsilon^i\phi^{(i)} = \frac{1}{2\pi}\int_a^{a^+}\sigma^{(i)}(\xi)\ln[(x-\xi)^2+y^2]^{1/2}d\xi + \frac{1}{2\pi}\int_a^{a^+}\gamma^{(1)}(\xi)\tan^{-1}\left(\frac{y}{x-\xi}\right)d\xi \tag{21}$$

where $\sigma^{(i)}$ and $\gamma^{(i)}$ are unknown source and vortex strengths, respectively, and $[a^-, a^+]$ represents the longitudinal extent along the x axis that the two ships occupy. The branch cut of the arctangent function should be chosen along the x axis with $x<\xi$. It is evident in Eq. (21) that the first term is even and the second odd in y. For matching with the inner solution, we consider first the even part. A three-term expansion in inner variables of the two-term outer solution is given by

$$[\epsilon\phi^{(1)}+\epsilon^2\phi^{(2)}]_{\text{even}} \cong \left[\phi^{(1)}(x,0)+\frac{\sigma^{(1)}}{2}|y| - \tfrac{1}{2}\phi^{(1)}_{xx}(x,0)y^2\right]+\left[\phi^{(2)}(x,0)+\frac{\sigma^{(2)}}{2}|y|\right] \tag{22}$$

Now, from Eqs. (6, 17, and 19), the even part of the two-term outer expansion of the three-term inner solution, when written in outer variables, is

$$[\epsilon\Phi^{(1)}+\epsilon^2\Phi^{(2)}+\epsilon^3\Phi^{(3)}]_{\text{even}} \cong \epsilon\left[f_1(x)+\frac{Q^{(2)}}{4H}|y| - \tfrac{1}{2}f_1''y^2\right]+\epsilon^2\left[f_2(x)+\frac{(f_1'A)'}{4H}|y|\right] \tag{23}$$

Comparing similar terms of Eqs. (22) and (23), we obtain the following immediately:

$$\sigma^{(1)}(x) = -\frac{\epsilon U}{2H}A'(x)$$

$$\epsilon f_1(x) = \frac{1}{2\pi}\int_{a^-}^{a^+}\sigma^{(1)}(\xi)\ell n|x-\xi|\,d\xi \tag{24}$$

$$\sigma^{(2)}(x) = \frac{\epsilon^2 U}{2H}(Af_1')'$$

$$\epsilon^2 f_2(x) = \frac{1}{2\pi}\int_{a^-}^{a^+}\sigma^{(2)}(\xi)\ell n|x-\xi|\,d\xi \tag{25}$$

Here, we observe, as far as the even solution is concerned, the presence of the second body serves merely to change the effective sectional area when compared with the result of a single body. Thus, the zero Froude-number sinkage force and trimming moment acting on each vessel can be obtained by Eqs. (6.12) and (6.13) of Tuck,[8] with only a minor modification in the definition of f_1. $V^{(2)}$ in Eq. (14) and $V^{(3)}$ in Eq. (19) still remain to be determined. These will have to come from the asymmetrical solution of the outer problem.

For the vortex-distribution integrals, we observe that, for small values of y,

$$\frac{1}{2\pi}\int_{a^-}^{a^+}\gamma(\xi)\tan^{-1}\left(\frac{y}{x-\xi}\right)d\xi = \frac{\operatorname{sgn}(y)}{2}\int_x^{a^+}\gamma(\xi)\,d\xi+\frac{y}{2\pi}\int_{a^-}^{a^+}\frac{\gamma(\xi)}{x-\xi}\,d\xi+O(y^3) \tag{26}$$

where the second integral is to be interpreted in the Cauchy principal-value sense. Hence the two-term inner expansion of the two-term outer solution is

$$[\epsilon\phi^{(1)}+\epsilon^2\phi^{(2)}]_{\text{odd}} \cong \left[\pm\frac{1}{2}\int_x^{a^+}\gamma^{(1)}(\xi)\,d\xi\right]+\left[\pm\frac{1}{2}\int_x^{a^+}\gamma^{(2)}(\xi)\,d\xi+\frac{y}{2\pi}\int_{a^-}^{a^+}\frac{\gamma^{(1)}(\xi)}{x-\xi}\right] \quad \text{as } y\to 0^{\pm} \tag{27}$$

while the two-term outer expansion of Eq. (18) takes the form

$$[\epsilon^2\Phi^{(2)}]_{\text{odd}} \cong \pm\epsilon^2[UC_0+V^{(2)}C_1]+\epsilon V^{(2)}y \tag{28}$$

Comparison of terms of similar nature in Eqs. (27) and (28) yields

$$\tfrac{1}{2}(\gamma^{(1)}(x)+\gamma^{(2)}(x)) = -\epsilon^2[UC_0+V^{(2)}C_1]' \tag{29a}$$

$$\epsilon V^{(2)}(x) = \frac{1}{2\pi}\int_{a^-}^{a^+}\frac{\gamma^{(1)}(\xi)}{x-\xi}\,d\xi \tag{29b}$$

Equation (29b) implies that $\gamma^{(1)}$ is $0(\epsilon)$, but the right-hand side of Eq. (29a) is $0(\epsilon^2)$. Hence, they can be consistent only when

$$\gamma^{(1)}(x) = V^{(2)}(x) = 0 \tag{30}$$

This implies that the second-order "cross-flow," which represents the extent of the unsymmetrical flux, is identically zero. Hence, Eq. (29a) immediately yields

$$\gamma^{(2)}(x) = -\epsilon^2 2U(dC_0/dx) \tag{31}$$

If we now proceed to match the three-term inner expansion of $(\epsilon\phi^{(1)}+\epsilon^2\phi^{(2)})_{\text{odd}}$ with the two-term outer expansion of $(\epsilon^2\Phi^{(2)}+\epsilon^3\Phi^{(3)})_{\text{odd}}$ we will obtain in closed form the following solution for $V^{(3)}(x)$:

$$V^{(3)}(x) = \frac{-U}{\pi}\int_{a^-}^{a^+}\frac{C_0'(\xi)}{x-\xi}\,d\xi \tag{32}$$

Therefore, Eqs. (14) and (19) now are given uniquely by:

$$\Phi^{(2)} = U\phi_0+f_2(x) \tag{33}$$

$$\Phi^{(3)} = -f_1'\phi_0-\tfrac{1}{2}f_1''Y^2+f_1''\phi_*+V^{(3)}\phi_1+f_3(x) \tag{34}$$

For the restrictions on $C_0'(\xi)$, in order for $V^{(3)}$ to exist, we refer the reader to Muskhelishvili.[9] We point out however, that sufficient conditions require that the vessels have pointed ends, and that the combined sectional area curve $A(x)$ has continuous second derivatives in $[a^-, a^+]$.

The matching process is now complete. One notices that to second order the inner potential assumes a flow pattern with equal stream velocities at both lateral infinities. Another significant point is that, to this order, only a strip-theory-type solution is necessary to obtain the interaction forces and moment, since the solution of Φ at successive sections do not interact among themselves until the third order through $V^{(3)}(x)$. Further, because of the symmetry of the boundary condition about the centerplanes, only the overlapping portion of the vessels will contribute to interaction forces and moment. This last point is consistent with what Tuck and Newman[1] (Sec. 3) observed when the limit of $d_c\to 0$ of the complementary (far-field) problem was taken.

It is worthwhile to point out that, if the orders of the terms in Eqs. (27) and (28) are not kept strictly, the following integral equation for $V^{(2)}$ results when one omits $\gamma^{(2)}$ on the left-hand side of Eq. (29a):

$$V^{(2)}(x)+\frac{1}{\pi}\int_{a^-}^{a^+}\frac{[UC_0+V^{(2)}C_1]'}{x-\xi}\,d\xi = 0 \tag{35}$$

which is similar to one considered previously by Newman.[10] Since the numerator in the integral is by analysis one order smaller than $V^{(2)}$, this is justifiable only when C_0 is $0(\epsilon)$ and C_1 is 0(1) with respect to the outer field. In fact, this would correspond to the case of very small under-keel clearance (cf. Taylor[11]), which is not considered here. For such a case, C_0' and C_1' would become discontinuous at the stern of the

leading ship and at the bow of the trailing ship, leading to concentrated loading in Eq. (35), which must be handled with caution.

Finally, we note in passing that the conclusion of $V^{(2)}=0$ is not altered by the inclusion of first-order free-surface effects. The formulation of the inner problems $\Phi^{(1)}$ and $\Phi^{(2)}$ remain unchanged. The first-order outer problem $\phi^{(1)}$ still will satisfy Laplace's equation, with the transverse variable y replaced by $(1-F_h{}^2)^{1/2}y$ (see Tuck[8]), where F_h is depth-Froude number. The first-order vortex strength, once again, cannot match with the second-order discontinuity in the potential defined by Eq. (18). The first-order source strength, however, will increase by a factor of $(1-F_h{}^2)^{-1/2}$ with a similar effect on the expression for $f_1(x)$. The analysis becomes more complicated if $\Phi^{(3)}$ and $\phi^{(2)}$ are included; the latter must satisfy Poisson's equation in the horizontal plane.

4. Interaction Forces and Moments

Since it is not possible to distinguish the two ships from each other in the outer problem, interaction forces and moments can be obtained only from the inner field. Furthermore, since $V^{(2)}=0$, Tuck's inner expansion[8] of the pressure field can be adopted. Thus, it follows that

$$C_p(x;Y,Z)=(p-p_\infty)/\tfrac{1}{2}\rho U^2=\epsilon p_1(x)+\epsilon^2[p_2(x)+P_2(x;Y,Z)]+0(\epsilon^3) \tag{36}$$

where

$$p_1(x)=2f_1'(x)/U \tag{37a}$$

$$p_2(x)=2f_2'/U-f_1'^2/U^2 \tag{37b}$$

$$P_2(x;Y,Z)=2\phi_{0x}-[(\phi_{0Y})^2+(\phi_{0Z})^2] \tag{37c}$$

Only terms up to the second order will be considered hereafter. Assuming centerplane symmetry, we note that p_1 and p_2 do not contribute any lateral force, although they enter into sinkage and trim calculations. Hence, the leading sway force and yaw moment are $0(\epsilon^3)$ and require the knowledge of ϕ_0 obtained by solving Eq. (7) with the conditions (9, 15a, and 15b). The lateral force on the jth ship Y_j can be obtained by integrating the proper component of pressure force over the hull:

$$\frac{Y_j}{\tfrac{1}{2}\rho U^2}=\int_{a_-^*}^{a_+^*}\oint_{S_j}\left[\frac{\partial\phi_0}{\partial x}-\frac{1}{2}\left\{\left(\frac{\partial\phi_0}{\partial N}\right)^2+\left(\frac{\partial\phi_0}{\partial\tau}\right)^2\right\}\right]N_Y(x,s)\,\mathrm{d}s\;\mathrm{d}x \tag{38}$$

where $[a_-^*, a_+^*]$ is the longitudinal extent occupied by the overlapping region, and τ represents a tangential unit vector on S_j. If the stern of the leading ship does not vanish as a point, $\partial\phi_0/\partial x$ is singular at $x=a_-^*$, unless both hull functions are stationary in x at this point. The pressure singularity can be interpreted as a delta function of intensity ϕ_0, or, alternatively, an integration by parts of the first term yields

$$\oint_{S_j}\frac{\partial\phi_0}{\partial x}N_Y\,\mathrm{d}s=\frac{\mathrm{d}}{\mathrm{d}x}\int_{S_j}\phi_0N_Y\,\mathrm{d}s-\int_{S_j}\phi_0\frac{\partial}{\partial x}[N_Ys'(\theta)]\,\mathrm{d}\theta-\int_{S_j}\left[N_Y\frac{\partial\phi_0}{\partial N}\frac{\partial\phi_0}{\partial\tau}\frac{R_\theta}{R}\right]\mathrm{d}s \tag{39}$$

Now, noting that $\partial\phi_0/\partial N$ is symmetric in Eq. (38), we finally obtain

$$\frac{Y_j}{\tfrac{1}{2}\rho U^2}=I(a_-^*)-\int_{a_-^*}^{a_+^*}Y_{2D}(x)\,\mathrm{d}x \tag{40}$$

where

$$I(x)=\oint_{S_j}\phi_0N_Y\,\mathrm{d}s \tag{41}$$

$$Y_{2D}(x)=\oint_{S_j}\phi_0\frac{\partial}{\partial x}(N_ys')\,\mathrm{d}\theta+\oint_{S_j}\frac{\partial\phi_0}{\partial\tau}\left(\phi_{0_N}\frac{R_\theta}{R}+\frac{1}{2}\phi_{0\tau}\right)N_y\,\mathrm{d}s \tag{42}$$

which does not involve any numerical differentiation of the derived quantity ϕ_0 in the longitudinal direction. In obtaining Eq. (40), we have assumed that the bows are pointed; hence, $I(a_+^*)=0$. Similar analysis for the yaw moment then yields

$$\frac{M_j}{\tfrac{1}{2}\rho U^2}=a_-^*I(a_-^*)-\int_{a_-^*}^{a_+^*}[I(x)+xY_{2D}(x)]\,\mathrm{d}x \tag{43}$$

5. Numerical Solution of the Inner Problem

A Fredholm integral equation of the second kind can be constructed to describe the unknown potential ϕ_0. What is presented in the following also can be applied to the perturbation potential $\tilde{\phi}$ associated with the problem for ϕ_1, with $\tilde{\phi}\equiv\phi_1-Y$. Only a change in the expression for the body boundary-condition will be necessary. If one applies Green's theorem to ϕ_0 and a "channel" Green function G, then for a point P on S_j, the following identity can be derived:

$$\pi\phi_0(P)=\oint_{S_{1U}S_2}\phi_0(Q)G_n(P;Q)\,\mathrm{d}s_Q-\oint_{S_{1U}S_2}v_nG\,\mathrm{d}s-A'(x)\ell n4 \tag{44}$$

where $G(P;Q)=G(Y-\eta,\,Z-\zeta)$ is the channel source function given by

$$G=\frac{1}{2}\ell n\left[\sinh^2\frac{\pi}{4H}(Y-\eta)+\sin^2\frac{\pi}{4H}(Z-\zeta)\right]+\frac{1}{2}\ell n\left[\sinh^2\frac{\pi}{4H}(Y-\eta)+\cos^2\frac{\pi}{4H}(Z+\zeta)\right] \tag{45}$$

In obtaining Eq. (44), it is necessary to note that $G\to\pi(Y-\eta)/2H-\ell n4$ as $|Y-\eta|\to\infty$.

Although the blockage constant C_0 was never used explicitly because of the absence of outer problem, we show below that it can be calculated from integrals over the body contours. Consider now the case in which the point P is in the fluid; the left-hand side of Eq. (44) is given by $2\pi\phi(P)$. Let $Y\to\pm\infty$. Then the first integral of Eq. (44) reduces to

$$\oint_{S_{1U}S_2}\phi_0(N\cdot\nabla G)\,\mathrm{d}s=\mp\frac{\pi}{2H}\oint_{S_{1U}S_2}\phi_0N_Y\,\mathrm{d}s \tag{46}$$

whereas the second integral becomes

$$\oint_{S_{1U}S_2}v_nG\,\mathrm{d}s=(\pi/2H)(A'|Y|\mp\oint_{S_{1U}S_2}v_n\eta\,\mathrm{d}s)-A'\ell n4 \tag{47}$$

By use of these asymptotic expressions in Eq. (44), and comparing the result with Eq. (15b), we obtain the following formula for C_0:

$$C_0=\frac{1}{4H}\left[\sum_{j=1}^{2}\lambda_jA_j'(x)-\oint_{S_{1U}S_2}\phi_0N_Y\,\mathrm{d}s\right] \tag{48}$$

where λ_j denotes the lateral distance of the centerplane of the jth body from the x axis. A similar analysis for ϕ_I will allow us to recover Sedov's formula[12] for C_I:

$$C_I = \frac{1}{4H}[A + \mu_{YY}] \qquad \mu_{YY} = \oint_{S_{IU}S_2} \phi_I N_Y \mathrm{d}s \tag{49}$$

where $\rho\mu_{YY}$ is now the lateral added mass of the combined bodies. From Eqs. (48) and (49), one notices that, to the outer field, the constants C_0 and C_I are $0(\epsilon^2)$ and $0(\epsilon)$, respectively, if ϕ_0 and ϕ_I are of the same respective order. However, as the under-keel clearance decreases, it is well-known that μ_{YY} increases rapidly.[13] By using an asymptotic formula given therein, one can show that C_I becomes 0(1) as the clearance-to-depth ratio changes to $0(\epsilon)$. The magnitude of C_0 also can be inferred similarly.

The integral equation, Eq. (44), can be handled conveniently by the method of discretization,[14] which leads to the following system of linear equations for the discrete values of ϕ_0 on $S_{IU}S_2$, ϕ_{0j}, $j=1,2,\ldots,M$:

$$\sum_{j=1}^{M} (-\pi\delta_{ij} + K_{ij})\phi_{0j} = D_i \qquad \delta_{ij} = \begin{cases} 1, & i=j \\ 0, & i\neq j \end{cases} \tag{50}$$

where

$$K_{ij} = \int_{(\eta_j,\zeta_j)}^{(\eta_{j+1},\zeta_{j+1})} G_N \mathrm{d}s$$

$$= \left\{ \tan^{-1}\left[\coth\frac{\pi}{4H}(Y_i-\eta)\tan\frac{\pi}{4H}(Z_i+\zeta)\right] \right.$$

$$\left. -\tan^{-1}\left[\tanh\frac{\pi}{4H}(Y_i-\eta)\tan\frac{\pi}{4H}(Z_i-\zeta)\right]\right\} \Big|_{(\eta_j,\zeta_j)}^{(\eta_{j+1},\zeta_{j+1})} \tag{51a}$$

$$D_i = \oint_{S_{IU}S_2} G(Y_i,Z_i;Q)\, v_n(Q)\mathrm{d}s_Q + A'\ell n4 \tag{51b}$$

Here (η_j,ζ_j), $j=1,\ldots M+1$, denotes the collection of points that provides a polygonal approximation of the body section. In the actual computation, the symmetry of solution about $z=0$ is exploited. The evaluation of K_{ij} and D_i occupies a major portion of the computation time for a typical problem.

We recall that Eqs. (40) and (43) require the inner solution in the overlapping region only. If the body has a fin-like appendage at the stern, corresponding to the presence of a rudder or skeg, it is reasonable to assume that a vortex sheet has shed from the trailing edge on such a fin. In the context of low-aspect-ratio lifting surfaces, such a vortex sheet has no upstream influence,[15] but its presence generates an unsymmetrical flow about the adjacent body in the nonoverlapping region. Newman and Wu[15] showed that the dynamic boundary condition on the sheet simply implies that the vorticity at the trailing edge is convected downstream. This type of inviscid wake model can be incorporated easily in the foregoing solution algorithm of ϕ_0. As an illustration, consider a typical section located downstream of a fin-like stern of ship 2 (Fig. 3). Eq. (44) becomes:

$$\pi\phi_0(P) = \oint_{S_I} \phi_0 G_N \mathrm{d}s - \int_{S_w} \Delta\phi_0(x;\eta,\zeta) G_N \mathrm{d}s$$

$$- \oint_{S_I} v_n G \mathrm{d}s - A_I'(x)\ell n4 \qquad \text{for } P\epsilon S_I \tag{52}$$

Here the second integral represents a dipole distribution on the wake surface. The strength is given by the "jump" in the potential corresponding to an upstream point on the same streamline at the trailing edge, i.e.,

$$\Delta\phi_0(x;\eta,\zeta) = \Delta\phi_0(a^*_-;\lambda_2,\tilde{\zeta}) \tag{53}$$

with

$$\eta = \lambda_2 + \int_{a^*_-}^{x} v(x;\lambda_2,\zeta)\mathrm{d}x \tag{54a}$$

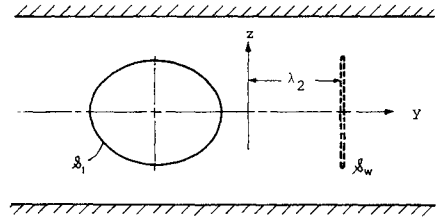

Fig. 3 Body section with wake vortex sheet.

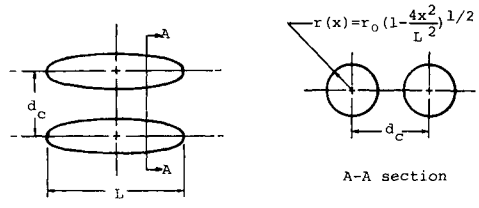

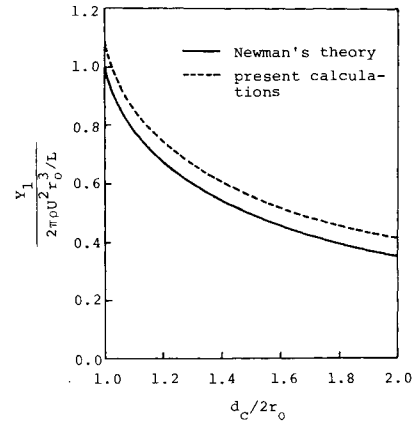

Fig. 4 Interaction force of two spheroids.

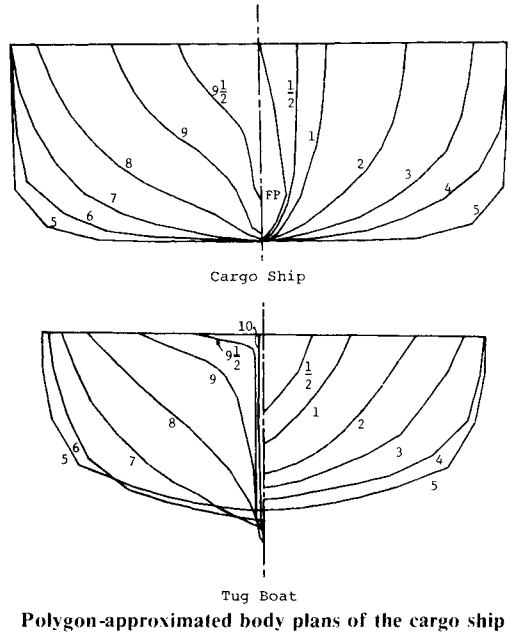

Fig. 5 Polygon-approximated body plans of the cargo ship and tug boat.

Table 1 Particulars of models used in calculations

Model identifier	Cargo liner	Tug	Model A	Model B
Length, LBP, meters	3.478	0.838	3.320	2.958
Length/beam	6.767	3.880	7.023	7.836
Beam/mean draft	2.700	2.570	2.848	2.373
C_B	0.590	0.486	0.701	0.761
Water-depth/draft	1.38	3.26	1.67	1.30

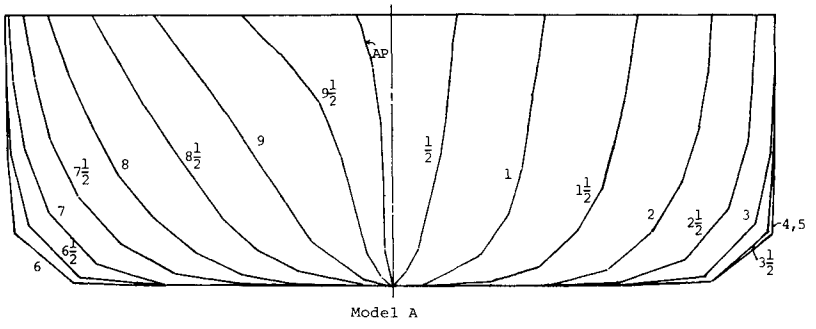

Model A

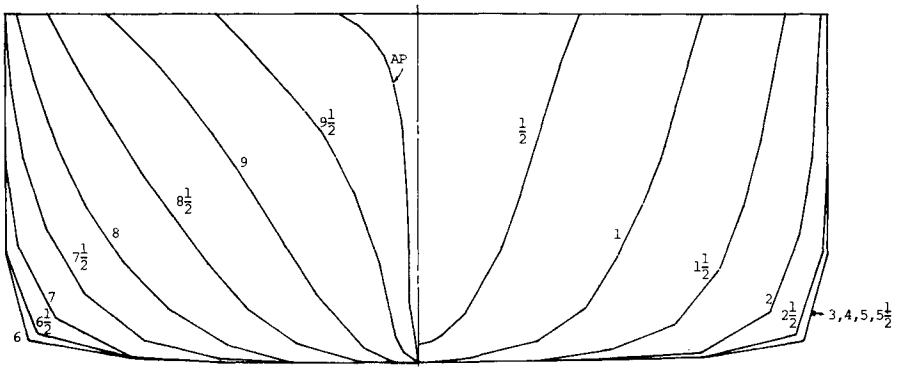

Model B

Fig. 6 Sway force and yaw moment on tug in steady motion.

$$\zeta = \tilde{\zeta} + \int_{a^*}^{x} w(x;\lambda_2,\zeta)\,dx \tag{54b}$$

where v and w are the solutions of Eq. (52) without the S_w term. Actual calculations show that such a wake vortex sheet has rather insignificant influence on the overall force and moment, at least for the cases investigated here.

6. Results and Discussion

A computer program based on the present theory has been developed for the evaluation of Eqs. (40) and (43). The interacting vessels can be of arbitrary form. The core subprogram consists of the solution algorithm for the inner problem ϕ_0 described in Sec. 5. Verifications of this subprogram were made by applying it to obtain C_l for a number of cylindrical shapes considered previously by others.[13] The overall programming then was checked by calculating the sway force on a spheroid moving near a wall in an otherwise infinite fluid. A closed-form solution of this was obtained earlier by Newman.[16] Figure 4 shows a comparison of the computed results with those of Newman. Each computed point was cross-checked by repeating the computations using Eq. (38). We note that the functional dependence of the calculated curve is in the same form as Newman's. The discrepancy is attributable to a difference in the approximate evaluation of the slender-body force integral.

The theory presented was next applied to two pairs of realistic ship hulls, for which experimental results in shallow water are available. The experiments were conducted by Dand at the National Physical Laboratory, England.[6,17] The particulars of the models were given in Table 1. The first pair consists of a cargo vessel and a tug boat. The length ratio of the two ships is 0.24. The fact that the models are of rather dissimilar size offers a stringent test on the practicability of the theory. The water-depth to draft ratios are 1.38 and 3.28 for the large and small ships, respectively. The nondimensional separation distance based on the larger ship length is 0.128. Polygon-approximated body plans of the two models are shown in Fig. 5. The cargo liner has a closed stern. The skeg and large rudder of the tug are approximated by a fin-like structure in the aftermost half-station. Computed results are shown with experimental data in Fig. 6. Here, one observes the rather satisfactory force prediction when the vessels are in abreast configuration. The predictions corresponding to small-overlap configurations are much less accurate, particularly when the tug is in the stern region of the cargo liner. Unquestionably, it is in such configurations that one would expect the slender-body theory to be less effective, since three-dimensional effects clearly play an important role in the inner flow-field. The large peak in the moment curve and the force reversal predicted by the theory at $x_0/L_2 = 0.8$ are caused by the 'absence' of the end-effect term in Eq. (40) by virtue of the fact that the stern of the tug has moved out of the overlapping region. Oscillations in the moment curve, although puzzling at first, are attributable to the fact that both the integrand and the limits of integration of Eq. (43) are functions of the stagger. The qualitative features of this curve agree well with the inner limits of the complementary outer theory investigated by Yeung.[18]

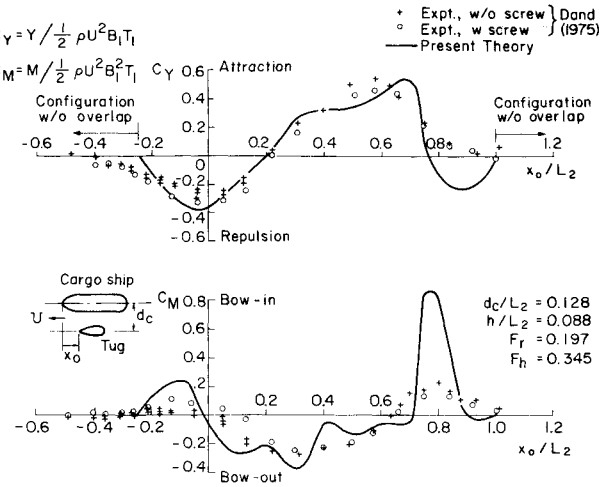

Fig. 7 Polygon-approximated body plans of models A and B.

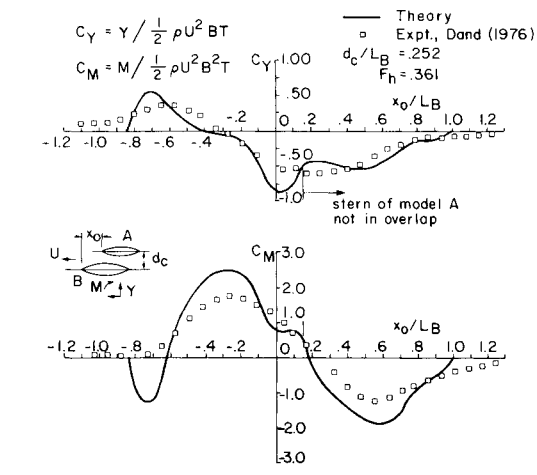

Fig. 8 Sway force and yaw moment on model A.

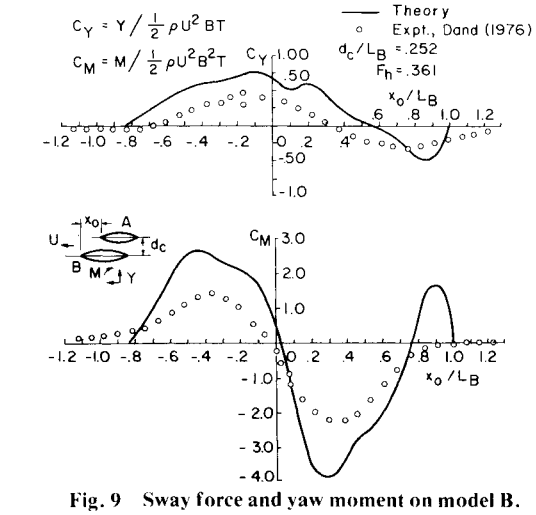

Fig. 9 Sway force and yaw moment on model B.

The second pair of vessels consists of a cargo ship and a tanker, designated by model A and B, respectively. The models are more similar in size, compared with the first pair considered: the length ratio being 0.839. Both are modeled by pointed bows with fin-like sterns. Their approximated body plans are shown in Fig. 7. Numerical results of the interaction force and moment are shown in Figs. 8 and 9, and are compared with the experimental data of Dand.[6] The experiments were conducted at two speeds; only the results of the lower speed case, $F_h = 0.361$, are cited. Theoretical predictions for model A (Fig. 8) appear to be quantitatively satisfactory, except when the vessel is in an ahead position with a small overlap. In this situation, the stern terms of Eqs. (40) and (43) play a much more dominant role than physically realized. It is of some interest to note that $x_0/L_B = 0.161$ corresponds to the particular stagger at which the two sterns coincide. Here the slopes of the theoretical curves will be discontinuous if the vessels do not have cusp ends. Figure 9 shows the corresponding comparison for the larger vessel, model B, with the measured data. The force and moment peaks are overestimated by a factor close to 2. Such a discrepancy can, in fact, be traced back to the validity of using a fin-like structure to represent the complicated geometry at the stern region.

7. Conclusions

Slender-body theory with a rigid free-surface assumption has been applied to predict the nearfield interaction of two ships. It was shown that, for the situation in which the water depth is of the same order of the vessel draft, the solution can be constructed, to second-order accuracy, by a stripwise calculation in the cross-flow plane without considering the outer problem. The inner problem, in general, requires the numerical solution of a coupled integral equation with specified flux conditions on both body sections.

Applications were made to two pairs of ship models for which experimental data in shallow water are available. Theoretical calculations appear to yield good qualitative agreement, particularly when the vessels have a large overlap. For small overlaps, three-dimensional effects near the bow and the stern regions are important, and clearly violate the assumptions taken in the theory.

From the quantitative viewpoint, the present strip theory tends to overpredict the sway force and yaw moment. This is to be expected, since the actual loading will be less severe owing to the three-dimensionality of the flow. The inclusion of a cross-flow viscous drag term, as is customarily performed in applying slender-body theory to a single vessel at a yaw angle, must be done with more scrutiny because of the nonuniformity of the cross flow in space.

Finally, it is worthwhile to point out that the computation time for such a mathematical model of ship interactions, although not as prohibitive as three-dimensional calculations, is sufficiently large so that its applications to real-time simulation appear to be impractical. Furthermore, extreme care also must be exercised in the preparation of the hull data to insure that the hull geometry is sufficiently smooth. The solution of the inner problem is found to be rather sensitive to any local irregularities.

Acknowledgment

The authors are grateful to the National Science Foundation for supporting this work, under grants GK43886X and ENG75-10308.

References

[1] Tuck, E. O. and Newman, J. N., "Hydrodynamic Interactions Between Ships," *Proceedings of the 10th Symposium on Naval Hydrodynamics*, Office of Naval Research, 1974, pp. 35-70.

[2] Wang, S., "Forces and Moment on a Moored Vessel Due to a Passing Ship," *Journal of the Waterways, Harbors, and Coastal Engineering Division, Proceedings of ASCE*, Vol. 101, Aug. 1975, pp. 247-258.

[3] Nowacki, H., "Über die Wechselseitigen Kraftwirkungen zwischen Schiffsahnlichen Tauchkörpern," *Schiff und Hafen*, Jahrg. 12, Heft 9, Sept. 1960, pp. 756-760.

[4] Norrbin, N. H., "Bank Effects on a Ship Moving Through a Short Dredged Channel," *Proceedings of the 10th Symposium on Naval Hydrodynamics*, Office of Naval Research, 1974, pp. 71-88.

[5] Collatz, G., "Potentialtheoretische Untersuchung der Hydrodynamischen Wechselwirkung zweier Schiffskörper," *Jahrbuch der Schiffbautechnischen Gesellschaft*, Band 57, 1963, pp. 281-329.

[6]Dand, I. W., "Hydrodynamic Aspects of Shallow Water Collisions," *Journal of RINA*, Nov. 1976, pp. 323-337.

[7]Hess, J. L. and Smith, A.M.O., "Calculation of Potential Flow about Arbitrary Bodies," *Progress in Aeronautical Sciences*, Vol. 8, 1967, pp. 1-137.

[8]Tuck, E. O., "Shallow-Water Flows Past Slender Bodies," *Journal of Fluid Mechanics*, Vol. 26, Sept. 1966, pp. 81-95.

[9]Muskhelishvili, N. I., *Singular Integral Equations*, 2nd ed., Wolters-Noordhoff, Groningen, The Netherlands (English Translation), 1958.

[10]Newman, J. N., "Lateral Motion of a Slender Body Between Two Parallel Walls," *Journal of Fluid Mechanics*, Vol. 39, Oct. 1969, pp. 97-115.

[11]Taylor, P. J., "The Blockage Coefficient for Flow About an Arbitrary Body Immersed in a Channel," *Journal of Ship Research*, Vol. 17, June 1973, pp. 97-105.

[12]Sedov, L. I., *Two-Dimensional Problems in Hydrodynamics and Aerodynamics*, John Wiley and Sons, New York, 1965.

[13]Flagg, C. N. and Newman, J. N., "Sway Added-Mass Coefficients for Rectangular Profiles in Shallow Water," *Journal of Ship Research*, Vol. 15, Dec. 1971, pp. 257-265.

[14]Hildebrand, F. B., *Methods of Applied Mathematics*, 2nd ed., Prentice-Hall, Englewood Cliffs, 1965.

[15]Newman, J. N. and Wu, T. Y., "A Generalized Slender-Body Theory for Fish-Like Forms," *Journal of Fluid Mechanics*, Vol. 57, March 1973, pp. 673-693.

[16]Newman, J. N., "The Force and Moment on a Slender Body of Revolution Moving Near a Wall," David Taylor Model Basin, Rept. 2127, 1965.

[17]Dand, I. W., "Some Aspects of Tug-Ship Interaction," Proceedings of 4th International Tug Convention, 1975, pp. 61-75.

[18]Yeung, R. W., "On the Interactions of Slender Ships in Shallow Water," to appear *Journal of Fluid Mechanics*, 1977.